SUPERSONIC FLOW FIELD SIMULATION IN PLANAR AND DOUBLE PLANAR DIVERGENT NOZZLES

Sidali HAIF[1], Hakim KBAB[2], Amina BENKHEDDA[3]

The main objective of the dual bell nozzle concept is to gain performance by the principle of self-adaptation for two operating regimes without mechanical activation. Planar double divergent nozzle (DDN) is a type of dual bell nozzle, having a rectangular cross section. The current study involved the numerical analysis of a Planar double divergent nozzle, and a planar nozzle with the same area ratio and the same length using ANSYS-Fluent software. The results of the analysis showed that there is a 0.05% weight reduction for the planar double divergent nozzle. The thrust increase is estimated at 06.37% and 42.00% in the low-altitude operating mode and transmission mode respectively for the planar double divergent nozzle.

Keywords: Dual Bell Nozzle (DBN), Planar Double Divergent Nozzle (DDN), ANSYS-Fluent, FORTRAN, Method Of Characteristics (MOC).

1. Introduction

Dual bell nozzles are considered a solution to maximize efficiency at high altitudes, while avoiding dangerous side loads at lower altitudes. A dual bell nozzle consists of two different contours, the first operates at low altitudes but the second is intended to operate at high altitudes. These two contours are connected by a junction point.

In 1949, Cowles and Foster [1] introduced the concept of the dual bell nozzle. The concept was patented by Rocketdyne in the 1960s. In 1994 Horn and Fisher [2] confirmed the feasibility of this nozzle by carrying out tests at Rocketdyne and in Europe by the Future European Space Transportation Investigations program; European Space Transport Investigation (FESTIP). They studied four combinations of contours to find the extension that offered the most favorable flow transition characteristics and high-altitude performance. The performance of the dual bell nozzles has been shown to be below the theoretical

[1] Laboratoire des Sciences Aéronautique, Institut d`Aéronautique et des Études Spatiales, Université Saad Dahlab Blida1, Algeria, e-mail: haifsidali06@gmail.com
[2] Laboratoire des Sciences Aéronautique, Institut d`Aéronautique et des Études Spatiales, Université Saad Dahlab Blida1, Algeria, e-mail: k71.hakim@gmail.com
[3] Laboratoire des Sciences Aéronautique, Institut d`Aéronautique et des Études Spatiales, Université Saad Dahlab Blida1, Algeria, e-mail: benkhedda90@hotmail.com

optimum due to the loss of suction drag in low altitude mode and non-optimal contour in high altitude mode. They found that even with such losses, a dual bell nozzle could provide sufficient thrust to carry 12.1% more payload than a conventional CD (Converging-Diverging) nozzle with the same expansion ratio. In 1999, Frey and Hagemann [3] studied various aspects of the design of the wall deflection and nozzle extension, focusing on the dependence of the transition behavior on the type of nozzle extension. In 2013, Génin et al. [4, 5] carried out experimental and numerical studies on dual bell nozzles for the evaluation of the heat flow distribution. For both modes of operation (Sea-Level Mode and High-Altitude Mode) and as a result they have shown that the thermal flux value increases in the region of the contour inflection. The separation of the flows at the level of the inflection increases this phenomenon. Under sea level conditions, the flow separates at the contour inflection in a controlled and symmetrical manner. Side load generation continues to decrease and thrust increases due to the low area ratio. During flight, ambient pressure decreases, resulting in an increase in NPR (Nozzle Pressure Ratio). At a certain altitude, the NPR transition is reached and the point of separation leaves the inflection of the contour and moves rapidly towards the exit of the nozzle. Thrust is improved due to the larger area ratio. They also tested a dual bell planar nozzle design under several cold and hot flow test conditions. Analysis of the shock at the contour inflection gave an idea of the shape and position of the separation front. In sea level mode, the numerical and experimental results were in good agreement for higher NPR values, the calculated separation position was located further upstream than that measured in the experiments. In 2016, Schneider and Génin [6] analyzed the effect of various turbulence models and feeding pressure gradients on the flow transition behavior in the dual bell nozzle. They found better results for Reynolds stress and Spalart-Allmaras model. In both 2013, 2014 and 2015, Verma et al. [7], [8], [9] carried out three experimental studies, one to study the effect of the Reynolds number on the transition behavior of a dual bell nozzle for tests inside a high altitude simulation chamber, the second to study the dependence of the transition behavior on ambient pressure fluctuations in a dual bell nozzle. The last to study unstable flow conditions during the sneak transition by performing a cold gas test on a dual bell nozzle subscale operating under sea level conditions. In the latter the results showed that the flow during the sneak transition was very unstable and was the main source of side loads generation. In 2016, Hamitouche et al. [10] studied the design of dual bell nozzles and evaluated several wall parameters and performances using the method of characteristics (MOC). In 2017, Kbab et al. [11] carried out a numerical and simulation study on dual bell nozzles. They proposed for the first time a TOP (Thrust Optimized Parabolic) profile for the basic nozzle. In 2021, George et al. [12] studied numerically the effect of inflection angle on flow in planar double divergent nozzles. It is deduced from

this that the side load, the flow model and the specific impulse of a planar double divergent nozzle strongly depend on the angle of inflection.

This study focused on the contour design and numerical analysis of a planar double divergent nozzle and a planar nozzle using commercial ANSYS-Fluent software. The two nozzles (planar double divergent nozzle and the planar nozzle) having the same area ratios and the same length. The flow pattern, thrust and specific impulse are studied for several pressure ratios. Both geometries are studied with similar boundary conditions.

2. Methodology

This section is intended to describe the method used to design the planar double divergent nozzle. The design of the planar double divergent nozzle is carried out in two parts:

2. 1. Design of the first contour (divergent base)

The first divergent is a contour of a two-dimensional supersonic nozzle with a sharp-edged throat that gives uniform parallel flow at the exit. The method of characteristic applied to the two-dimensional isentropic flow of an ideal gas was used for the design of a supersonic planar nozzle. A sketch of a typical nozzle designed in this manner is shown in Fig. 1.

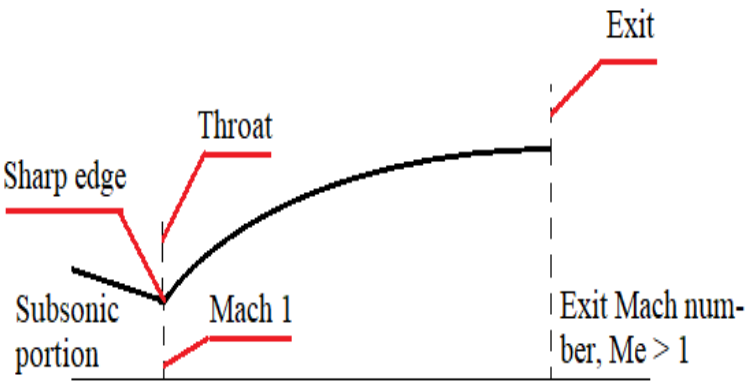

Fig. 1. Sharp-edged-throat supersonic nozzle.

The nomenclature for the nozzle is given in Fig. 2.

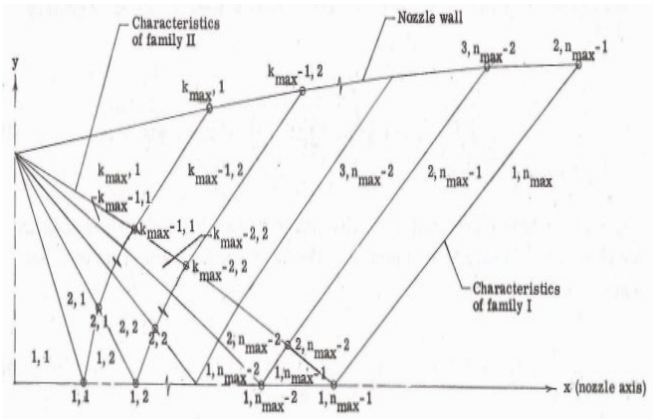

Fig. 2. Nomenclature and wave diagram for supersonic nozzle with sharp-edged throat [13].

Each small region is denoted by two index variables k and n, where k is a variable index for the characteristics of family II and n is a variable index for the characteristics of family I .

The equations and calculation procedures required to design the nozzle contour are as follows:

$$x_{k,n} = \frac{\left(y_{k+1,n+1} - m_{II} x_{k+1,n-1}\right) - \left(y_{k-1,n} - m_I x_{k-1,n}\right)}{m_I - m_{II}} \tag{1}$$

$$y_{k,n} = y_{k-1,n} + m_I \left(k_{k,n} - x_{k-1,n}\right) \tag{2}$$

$$m_I = \tan\left(\frac{u_{k,n} + u_{k-1,n+1}}{2} + \frac{\varphi_k + \varphi_{k-1}}{2}\right) \tag{3}$$

$$m_{II} = -\tan\left(\frac{u_{k,n} + u_{k+1,n}}{2} - \frac{\varphi_k + \varphi_{k+1}}{2}\right) \tag{4}$$

m_I : represent the slope for characteristics of family I

m_{II} : slope for characteristics of family II

$$u_{k,n} = \arcsin\left(\frac{1}{M_{k,n}}\right) \tag{5}$$

$$\varphi_k = \left(k-1\right)\Delta v \tag{6}$$

u : Mach angle

φ : Flow angle

$$M_{k,n} = \sqrt{\frac{\left(\frac{2}{\gamma+1}\right) M^{*2}_{k,n}}{1-\left(\frac{\gamma-1}{\gamma+1}\right) M^{*2}_{k,n}}} \tag{7}$$

The waves of family *II* extend beyond the region where the two families exist and cut the contour of the nozzle, which is shaped so as to cancel these waves. For the nozzle contour points, we solve the following set of equations: equation (1), (2) and $k = k_{\max}$. For more details, see Reference [13].

2. 2. Design of the second contour (nozzle extension)

The contour of the second divergent (nozzle extension) is a polynomial. This is achieved using the direct method of characteristics [14].

2. 3. Convergent part design

In this study, we relied on the ANSYS-Fluent software for numerical analysis and since it's in ANSYS-Fluent simulation the inlet (boundary condition) should be in the nozzles inlet not in the throat nozzles. So we added the convergent part before the throat section. The role of the convergent part, is to accelerate the flow out of the chamber, reaching the velocity of sound at the throat (M=1). The method used for the design of the convergent part contour is Rao's method [15]. This method uses circular arcs and the throat radius to design the contour. Equations 8 and 9 yield the coordinates for points along the converging section. Rao developed these relationships through experimental data. Rao's method was commonly used in the 1950's for rocket nozzle design.

$$x = 1.5R_{th}\cos\theta \tag{8}$$

$$y = 1.5R_{th}\sin\theta + 2.5R_{th} \tag{9}$$

Where R_{th} is the throat radius and $-130 \le \theta \le -90$ degrees.

With x and y represent the coordinates of the points along the convergent section. The Figure. 3 shows the profile of nozzle convergent part obtained by the FORTRAN program, which depends on both equations 8 and 9.

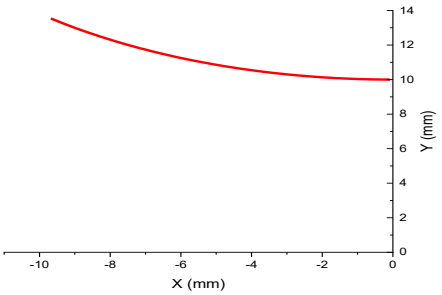

Fig. 3. Profile of nozzle convergent part.

3. Results

Using the FORTRAN program, which depends on the previous equations, we created the following:

- A planar nozzle with an exit Mach number of 2.0 and a length of 16.87 mm (The nozzle with which we compare our design).

- A planar double divergent nozzle with an exit Mach number for the first divergent (divergent base) equal to 1.5 and a second divergent (extension) extended to achieve the same length and same section ratio of the planar nozzle (see Fig. 4). We took an area ratio $\frac{A_e}{A_t} = 1.6875$ in both configurations.

With $\frac{A_e}{A_t}$: the area at exit the nozzle /throat area.

For the profile of the second divergent we have chosen two polynomials as follows:

- The polynomial curve of the first degree $Ax + B$. (Planar double divergent nozzle 1)

- The polynomial curve of the second degree $A + Bx + Cx^2$. (Planar double divergent nozzle 2)

Whose constants are calculated from the initial conditions.

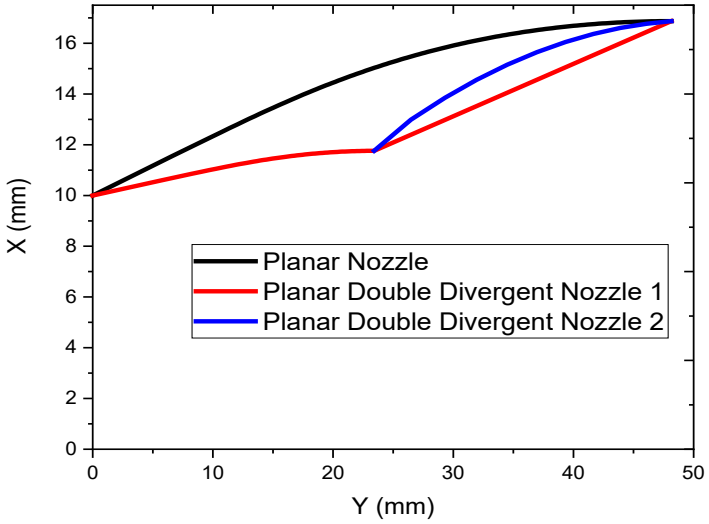

Fig. 4. Profile nozzles (planar nozzle and planar double divergent).

Figs. 5 and 6 presents the profile (in red) of the planar double divergent nozzle 1 and 2 respectively carried out by our computer code with its mesh (in green). The second degree polynomial constants are respectively:

A = -0.02350093, B = +0.6757153 and B = -0.06655531

The first degree polynomial constants are respectively:

A = 0.2067152 and B = 0.6918730

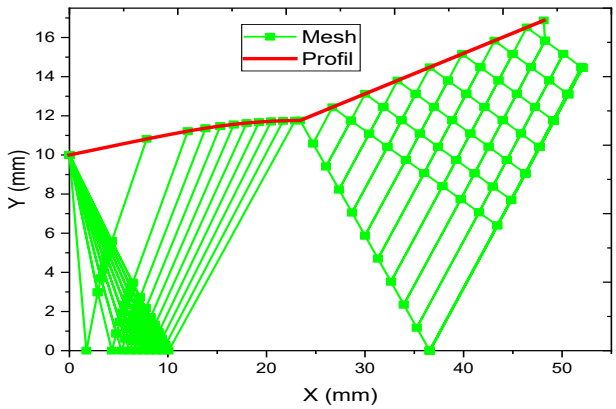

Fig. 5. The obtained planar double divergent nozzle 1 nozzle contour.

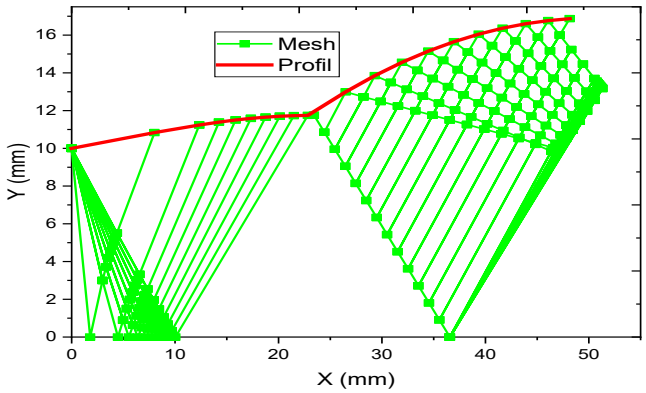

Fig. 6. The obtained planar double divergent nozzle 2 nozzle contour.

Table 1 represents the surface comparison. It is noted that the planar double divergent nozzle 1 is 0.051% lighter than the planar nozzle. As for the second nozzle, we notice an increase in weight by 0.226. We conclude that there are greater fuel savings for the planar double divergent nozzle. We have calculated the area of both nozzles to express the weight for the purpose of comparison.

Table 1

Nozzle area comparison.

	Planar Nozzle	Planar Double Divergent Nozzle 1	Planar Double Divergent Nozzle 2
Area (m^2)	0.09752	0.09747	0.09774
Weight gain%	0.00	0.051	-0.226

3. 1. Numerical simulations

In this part, a numerical analysis is performed on the flow through planar double divergent and planar nozzle. All geometries are studied under similar boundary conditions. Flow analysis is performed. Numerical analysis is performed on 2D planar models using the commercial ANSYS-Fluent software. The k-ω SST model was used as the turbulence model. The baseline solver was selected as a double-precision density-based coupled solver with Implicit Time Integration. Least-square cell-based gradient is used for spatial discretization in which the solution was assumed to vary linearly was used and a second-order upwind scheme was used for interpolating the values of pressure, momentum, turbulent kinetic energy, specific dissipation rate and energy. The computational analysis was conducted under steady conditions. The initialization for steady-state

problem was done using full multigrid (FMG) initialization to get the initial solution, and the inlet boundary was provided to give the reference value. Sutherland equation is used for calculating the viscosity of air.

Figures 7 and 8 represent the evolution of the Mach number along the wall of the planar double divergent nozzle 1 and 2 receptively. We note that there is a difference in the results obtained by the program and simulation at the beginning of the nozzle from the proximity of the throat. This is due to the distance of the calculation points in the program. See Fig. 5 and 6. There is an increase in the wall Mach value of up to 1.9 for planar double divergent nozzle 1 and stability at this value. As for the planar double divergent nozzle 2, we notice an increase in the value of the wall Mach up to 2.3, then a decrease to the value of 1.6.

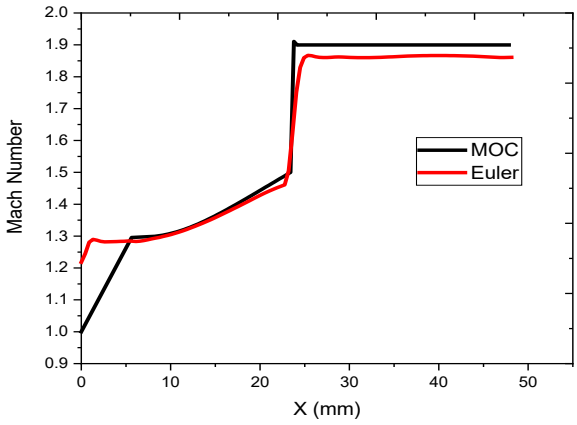

Fig. 7. Comparison between the wall MACH calculated by MOC and numerical simulation for Planar Double Divergent Nozzle 1.

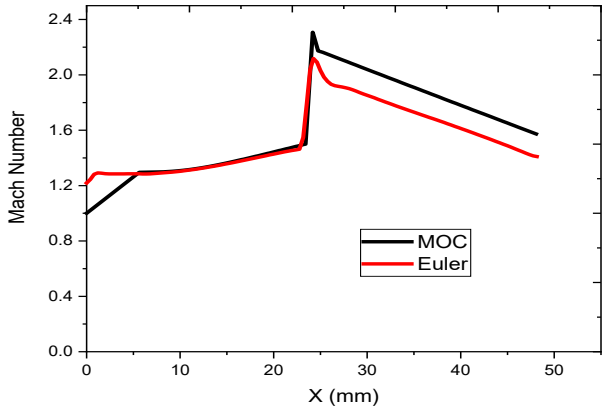

Fig. 8. Comparison between the wall MACH calculated by MOC and numerical simulation for Planar Double Divergent Nozzle 2

The wall pressure ratio (wall pressure/total pressure) distribution on Planar Double Divergent Nozzle 1 and 2 calculated by MOC and numerical simulation for is presented in Fig. 9 and 10. We note that in both nozzles 1 and 2, there are two phases of wall pressure reduction. In the first phase we observe a low wall pressure of 0.13 for planar double divergent nozzle 1 and 0.06 for planar double divergent nozzle 2. In the second phase, we notice that there is a stability in the wall pressure ratio at 0.13 with respect to planar double divergent nozzle 1, as for planar double divergent nozzle 2, there is a rise in wall pressure that reaches 0.25. There is also a noticeable convergence between the results obtained by the program (MOC) and simulation (Euler) results in the case of planar double divergent nozzle 1. While planar double divergent nozzle 2 there is a slight difference.

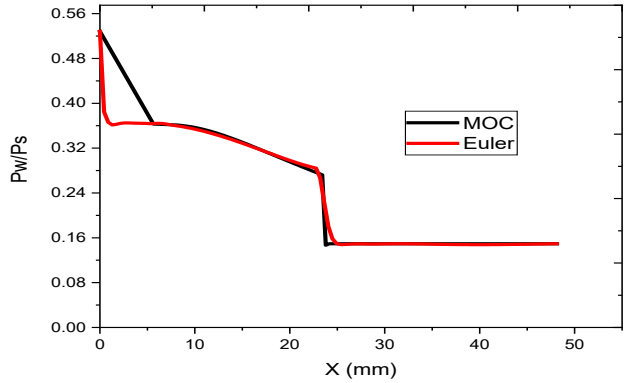

Fig. 9. Comparison between the wall pressure ratio calculated by MOC and numerical simulation for Planar Double Divergent Nozzle 1.

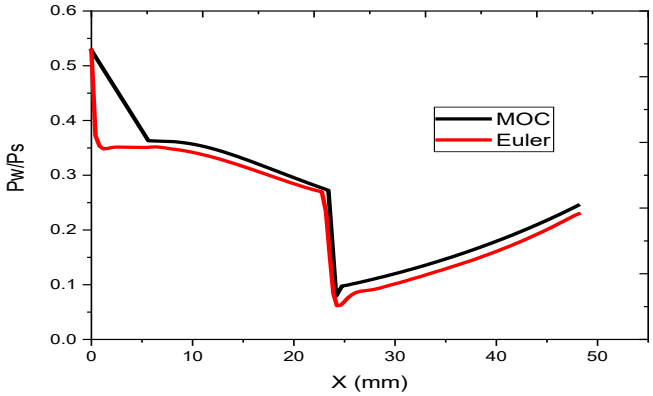

Fig. 10. Comparison between the wall pressure calculated by MOC and numerical simulation for Planar Double Divergent Nozzle 2.

Table 2 shows the thrust of nozzles 1 and 2 in high altitude mode. We notice a noticeable superiority of planar double divergent nozzle 1 by an estimated rate of 0.386% over planar double divergent nozzle 2, and this is what makes us rely on planar double divergent nozzle 1 in the rest of this study.

Table 2

Thrust comparison for the two nozzles in high altitude regimes.

	Planar Double Divergent Nozzle 1	Planar Double Divergent Nozzle 2	Thrust gain (%)
Thrust (N)	15570.62	15510.57	0.386

Figure 11 illustrates the mathematical-physical model, the boundary conditions and the mesh adopted for planar double divergent nozzle. The ambient conditions around the nozzle were modeled by applying a computational domain of $30R_{th}$ in the x-direction by $20R_{th}$ in the y-direction.

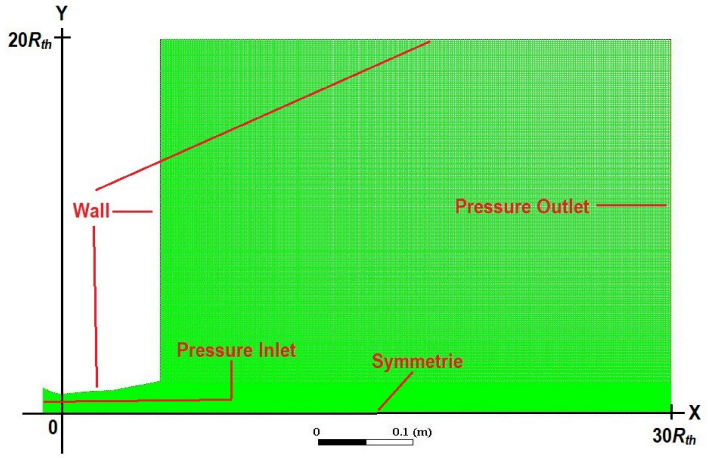

Fig. 11. The mathematical-physics model and the boundary conditions.

Tab. 3 represents number of the Nodes and Elements for planar double divergent nozzle obtained by ANSYS-ICEM.

Table 3

Nozzle gird information

	Planar double divergent nozzle
Nodes	95701
Elements	95000

Tab. 4 represents the boundary conditions values for the planar double divergent nozzle and planar nozzle. In order to reproduce the physics of the studied problem accurately, the total feeding pressure was kept constant, while the ambient pressure was changed (NPR) in this order: NPR=2.20 (low altitude mode, overexpansion), NPR= 2.90 (transient operating mode), NPR=7.83 (adapted

operating mode) and NPR=12.00 (Under-expansion). With NPR represent the total feeding pressure / the ambient pressure.

Table 4

Boundary conditions values.

	Planar double divergent nozzle	Planar nozzle
Gauge Total Pressure (Pa)	120000	120000
Supersonic/Initial Gauge Pressure (Pa)	120000	120000
Total Temperature (K)	330	330

Fig. 12 to Fig. 15 below represent the evolution of the Mach number along the wall of the both nozzle for deferential pressure ratio (NPR).

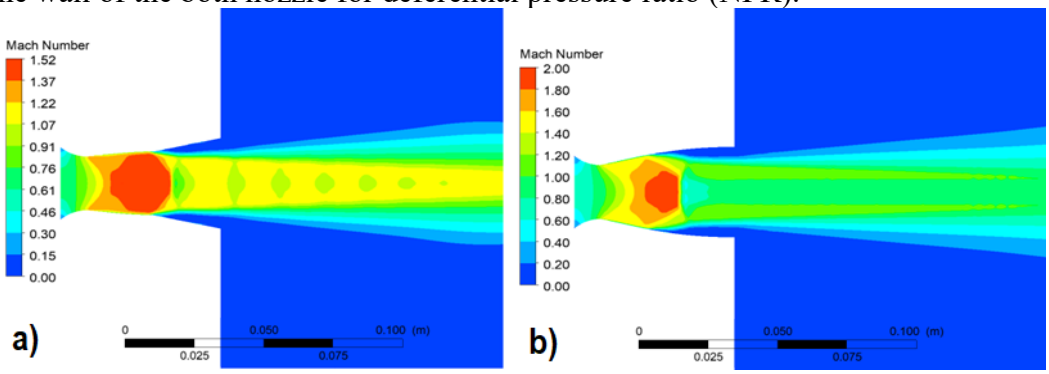

Fig. 12. Iso-Mach contour of the planar double divergent nozzle (a) and planar nozzle (b) for NPR=2.20.

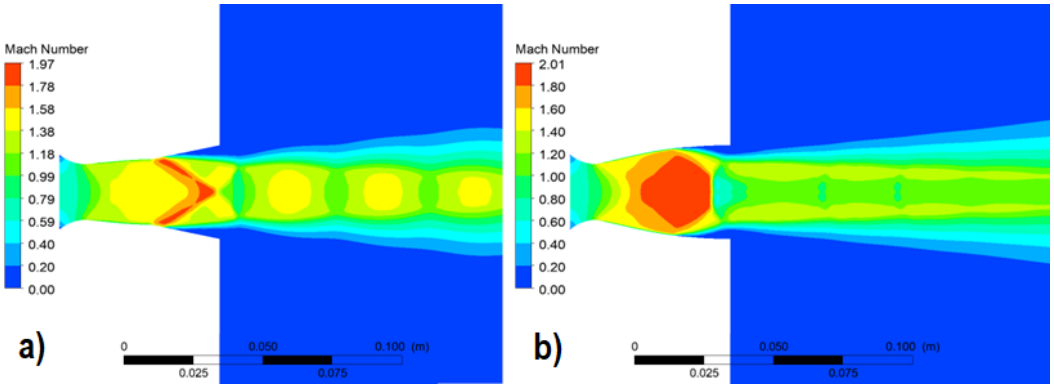

Fig. 13. Iso-Mach contour of the planar double divergent nozzle (a) and planar nozzle (b) for NPR=2.90.

For the NPR=2.20 (low altitude mode) we note that there is a separation of the flow in each of the nozzles. The separation of the flow occurs at the level of the inflection point (imposed separation) in the case of the planar double divergent nozzle.

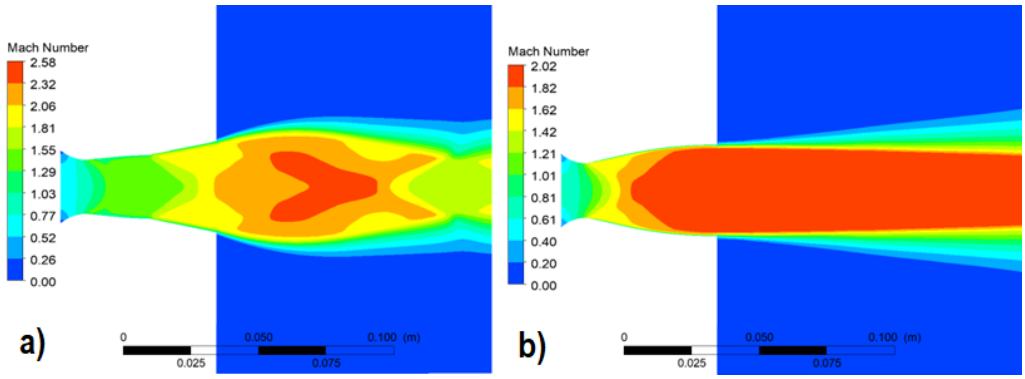

Fig. 14. Iso-Mach contour of the planar double divergent nozzle (a) and planar nozzle (b) for NPR=7.83.

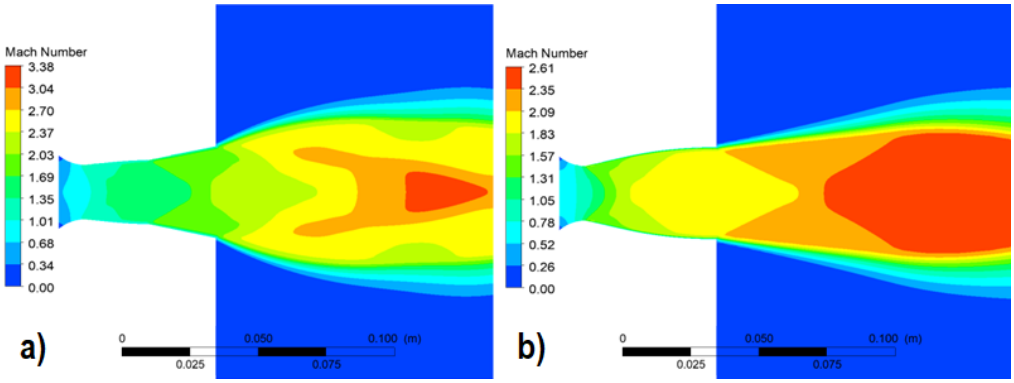

Fig. 15. Iso-Mach contour of the planar double divergent nozzle (a) and planar nozzle (b) for NPR=12.00.

This reduces side loads in low altitude mode in the case of a planar double divergent nozzle. For the NPR=2.90 (transient operating mode) there is no difference in flow separation in both nozzles. For the NPR=7.83 (adapted operating mode) we note the adaptation of the planar nozzle with this altitude, this is because the nozzle is designed for $M = 2.0$ and NPR = 7.83. For the NPR=12 (Under-expansion) there is an expansion of the flow in both nozzles.

Table 5

The thrust of the planar double divergent nozzle and the planar nozzle for deferential pressure ratio (NPR).

	Thrust (N)		
NPR	Planar Nozzle	Planar Double Divergent Nozzle	Thrust gain (%)
2.20	0640.22	0681.05	06.37
2.90	0731.22	1038.32	42.00
7.83	1544.32	1551.45	00.46
12.0	1661.10	1671.66	00.94

Tab. 5 represents the thrust delivered by the planar double divergent nozzle and the planar nozzle for NPR = 2.20, 2.90, 7.83 and 12.00 Note for NPR = 2.20 and 2.90 the planar double divergent nozzle delivers a significant thrust compared to the planar nozzle at an estimated rate of 06.37% and 42.00%

respectively. Finally for NPR = 7.83 and 12.00 the thrust of the Planar double divergent nozzle and the Planar nozzle is almost equal; this is due to the same area ratio of the two nozzles.

5. Conclusions

This research allowed us to study the performance of the planar double divergent nozzle compared to the planar nozzle. The current study involved the numerical analysis of a planar double divergent nozzle, and a planar nozzle with the same area ratio and the same length using ANSYS-Fluent software. The results of the analysis showed that there is a 0.05% weight reduction for the planar double divergent nozzle. The thrust increase is estimated at 06.37% and 42.00% in the low-altitude operating mode and transition mode, respectively, for the planar double divergent nozzle. For the low altitude mode the separation of the flow occurs at the level of the inflection point (imposed separation) in the case of the planar double divergent nozzle. This reduces side loads in low altitude mode in the case of a planar double divergent nozzle. For NPR = 7.83 and 12.00 the thrust of the planar double divergent nozzle and the planar nozzle is almost equal.

R E F E R E N C E S

[1]. *F. B. Cowles and C. R. Foster,* (1949). Experimental study of gas-flow separation in overexpanded exhaust nozzles for rocket motors (No. JPL-PR-4-103).

[2]. *M. Horn and S. Fisher,* "Dual-bell Altitude Compensating Nozzles", Pennsylvania State Univ., NASA Propulsion Engineering Research Center, **Vol. 2**, 1993.

[3]. *M. Frey and G. Hagemann,* "Critical Assessment of Dual-Bell Nozzles", Journal of Propulsion and Power, **Vol. 15**, no. 1, 1999, pp. 137-143

[4]. *C. Genin, R. H. Stark and D. Schneider,* "Transitional Behavior of Dual Bell Nozzles: Contour Optimization", in 49th AIAA/ASME/SAE/ASEE Joint PropulsionConference, 2013, pp. 3841

[5]. *C. Génin, A. Gernoth and R. Stark*, "Experimental and Numerical Study of Heat Flux in Dual Bell Nozzles", Journal of Propulsion and Power, **Vol. 29**, no. 1, 2013, pp. 21-26

[6]. *D. Schneider and C. Génin,* "Numerical Investigation of flow transition behavior in Cold Flow Dual-Bell Rocket Nozzles", Journal of Propulsion and Power, **Vol. 32**, no. 5, 2016, p. 1212-1219

[7]. *S. B. Verma, R. Stark and O. Haidn*, "Reynolds Number Influence on Dual-Bell Transition Phenomena", Journal of Propulsion and Power, **Vol. 29**, no. 3, 2013, p. 602-609

[8]. *S. B. Verma, R. Stark and O. Haidn*, "Effect of ambient pressure fluctuations on Dual-Bell Transition Behavior", Journal of Propulsion and Power, **Vol. 30**, no. 5, 2014, pp. 1192-1198

[9]. *S. B. Verma, A. Hadjadj and O. Haidn*, "Unsteady Flow Conditions During Dual-Bell Sneak Transition", Journal of Propulsion and Power, **Vol. 31**, no. 4, 2015, pp. 1175-1183

[10]. *T. Hamitouche, M. Sellam, H. Kbab, S. Bergheul, L. Lagab,* "Design and Performances of the Dual-Bell Nozzle", in IEEE Aerospace Conference, MT, USA, 2016.

[11]. *H. Kbab, M. Sellam, T. Hamitouche, S. Bergheul and L. Lagab*, "Design and Performance Evaluation of a Dual Bell Nozzle", Acta Astronautica, **Vol. 130**, no. January, 2017, pp. 52-59

[12]. *J. George, P. P. Nair, S. Soman, A. Suryan and H. D. Kim,* "Visualization of Flow Through Planar Double Divergent Nozzles by Computational Method", Journal of Visualization, **Vol. 24**, no. 4, 2021, pp. 1-22

[13]. *Micbael, R. and L. Goldman*, "Computer program for Design Of Two-Dimensional Supersonic Nozzle with Sharp-Edged Throat", NASA TM X-1502, 1963.

[14]. *M. J. Zukrow and J. D. Hofman,* "Gas Dynamics", John Wiley & Sons, New York, 1976.

[15]. *Devyn Yoshio Kapukawai Uyeki*, A Design Method for a Supersonic Axisymmetric Nozzle for Use in Wind Tunnel Facilities, MSc Thesis, Dan José University, 2018